Electronic noise in a constant voltage anemometer

Julien Weiss[a)]
Institut für Aerodynamik und Gasdynamik, Universität Stuttgart, 70550 Stuttgart, Germany

Geneviève Comte-Bellot[b)]
Centre Acoustique, LMFA, Ecole Centrale de Lyon, 69134 Ecully, France

The electronic noise and the signal-to-noise ratio in a constant voltage anemometer (CVA) are analyzed in terms of the main constitutive elements of the circuit. It is shown that the output voltage due to electronic noise decreases with the wire resistance, permitting one to know the noise upper limit by using the results of the unheated wire. The noise power spectrum increases at high frequencies as f^2, like in other anemometers, because of the need to compensate for the thermal lag of the hot wire, thus leading to a reduced signal-to-noise ratio at high frequencies. Explicit formulas are given in terms of wire, CVA, and flow quantities. Measurements of electronic noise in a CVA prototype confirm the theoretical analysis and illustrate some interesting issues concerning measurements of noise and low levels of flow fluctuations. © *2004 American Institute of Physics.*
[DOI: 10.1063/1.1711147]

I. INTRODUCTION

The constant voltage anemometer (CVA) is a recent type of hot-wire anemometer developed by Sarma.[1,2] It presents several valuable attributes for flow fluctuation measurements: Easy mode of operation, high bandwidth, stability, and insignificant cable capacitance effects.[2,3] In particular, the CVA has been shown to be especially advantageous for measurements of high-speed transitional and turbulent boundary layers.[3–5] Recent developments include a procedure for automatic stepping of overheat for measurement in short duration wind tunnels.[6]

For every measurement technique, the signal-to-noise ratio is a very important parameter since it determines the lowest signal that can be resolved. In analog systems, like hot-wire anemometers, the major sources of noise consist of the electronic noise generated by the operational amplifier and the thermal noise associated with the resistive components in the circuit. A theoretical analysis of the signal-to-noise ratio in the constant temperature anemometer (CTA) and in the constant current anemometer (CCA) has been performed by Freymuth.[7,8] In both cases, the hot wire was included in a Wheatstone bridge. The electronic noise was found to lead to a severe decrease of the signal-to-noise ratio at high frequencies, because of the need to compensate for the thermal inertia of the hot wire. In particular, Freymuth showed that at high frequency, the power spectrum of electronic noise rises like f^2, where f is the frequency, for both a CTA and CCA, so that there is always a frequency above which the noise dominates. This frequency can, in fact, limit the usable bandwidth in the measurement of low turbulence levels, as the turbulence spectra fall off rapidly with the frequency, according to f^{-1} or even $f^{-5/3}$ laws.[9–11] Bestion *et al.*[12] compared the noise performance of a CCA and CTA in high-speed flows and arrived at the conclusion that the two systems are basically equivalent, thus corroborating the theoretical work of Freymuth.[7,8]

Earlier references on the CVA considered the electronic noise only incidentally but showed that this new type of anemometer presents a lower level of noise when compared to other systems.[2,3,5] However, these results sometimes exhibited differences when noise spectra were compared. Therefore, the goal of the present article is to give a thorough analysis of the electronic noise and the signal-to-noise ratio in the CVA.[13]

The article is organized as follows: In Sec. II, the CVA output voltage due to electronic noise is established with the help of circuit equations derived by Sarma.[2] The signal-to-noise ratio is then obtained by comparing the anemometer response to flow fluctuations with the electronic noise. In Sec. III, experimental data confirming the theoretical results are presented. Finally, the present results, as well as specific issues concerning the measurement of electronic noise and low turbulent signals, are discussed in Sec. IV.

II. THEORETICAL ANALYSIS

A. Constant voltage anemometer circuit

A schematic diagram of the CVA is available in Sarma.[2] Like in typical op-amp circuits, the noise voltage at the circuit output is due to the thermal noise which occurs across the resistors composing the circuit, as well as the electronic noise in the op-amp itself.[14,15] The output noise voltage can thus be calculated by modeling all resistors by a perfect noiseless resistance in series with a fluctuating voltage source, and by modeling the op-amp noise with a finite number of noise sources.

Figure 1 shows the circuit obtained when this method is applied to the CVA circuit of Sarma.[2] Noise voltage sources

[a)]Present address: Department of Mechanical Engineering and Materials Science, Duke University, Durham, NC 27708; electronic mail: julien.weiss@duke.edu
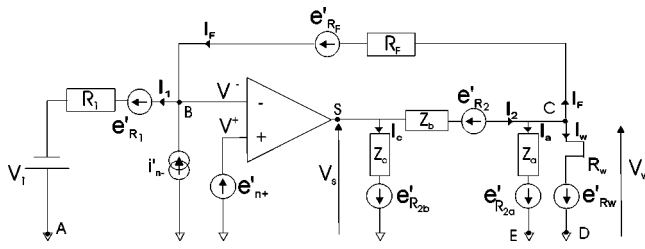[b)]Electronic mail: genevieve.comte-bellot@ec-lyon.fr

FIG. 1. CVA model including Nyquist–Johnson noise sources.

are included in the original circuit to model the thermal noise produced by the resistors. Reactive elements are assumed noiseless. The electronic noise in the op-amp is modeled by the noninverting input noise voltage e'_{n+} and the inverting input noise current i'_{n-}. This is a typical way of modeling the noise in amplifier circuits even if a large number of op-amps are used to build a complex amplifier network.[14,15]

In addition, several remarks must be considered:

(1) The time constant of the wire in the CVA is compensated by a resistor–capacitor (RC) T network. To simplify the analysis, this T network is transformed to its equivalent Π network.[2]
(2) The resistances R_a and R_b of the original circuit are renamed, respectively, R_{2a} and R_{2b} in Fig. 1.
(3) According to Sarma,[2] R_2, Z_a, Z_b, and Z_c are related to R_{2a} and R_{2b} by

$$R_2 = R_{2a} + R_{2b},$$

$$Z_a = R_{2a}\left(1 + \frac{1}{T_c s}\right),$$

$$Z_b = R_2(1 + T_c s),$$

$$Z_c = R_{2b}\left(1 + \frac{1}{T_c s}\right),$$

$$T_c = \frac{C R_{2a} R_{2b}}{R_2},$$

where s is the Laplace variable and T_c is the time constant compensation included in the CVA.

(4) The resistance R_d, which is in parallel with R_2 in the original circuit, introduces a damping term that limits the gain at very high frequency. Since R_d is much larger than R_2, its thermal noise will be neglected.

Typical values of the different resistors involved in the circuit are given by Sarma:[2] $R_1 = 1500\,\Omega$, $R_F = 300\,\Omega$, $R_2 = 100\,\Omega$, and $R_w \simeq 5\,\Omega$.

The different noise sources in Fig. 1 are related to the resistance and temperature of the corresponding resistors by the Nyquist–Johnson expressions: $\overline{e'^2_{R_1}} = 4kT_0 R_1 \Delta f$, $\overline{e'^2_{R_F}} = 4kT_0 R_F \Delta f$, $\overline{e'^2_{R_{2a}}} = 4kT_0 R_{2a} \Delta f$, $\overline{e'^2_{R_{2b}}} = 4kT_0 R_{2b} \Delta f$, $\overline{e'^2_{R_2}} = 4kT_0 R_2 \Delta f$, and $\overline{e'^2_{R_w}} = 4kT_w R_w \Delta f$. In these relations, $k = 1.38 \times 10^{-23}$ J/K is Boltzmann's constant, T_0 is the room temperature, T_w is the hot-wire temperature, and Δf is a frequency interval. It is assumed that the noise in each component is independent of the frequency (white noise). As

discussed by Freymuth,[7] the usual increase of noise in electrical components at low frequency (pink noise) is not of primary importance for hot-wire anemometry.

It should be noted that the model in Fig. 1 does not show the totality of the CVA circuit which is proprietary of Tao Systems Inc.[1,2] Nevertheless, the authors believe that the present simplified model is sufficient to understand the effect of electronic noise and its consequence on the signal-to-noise ratio of the anemometer. As will be shown in a further section, experimental data support the present approach very well.

B. Governing equations

The following analysis is performed in the frequency domain. Lower case variables written with a prime denote small fluctuating quantities and the same variables without a prime denote the spectral density of the corresponding quantity. For example, if $e'(f)$ is a small voltage fluctuation, then $e(f)$ is the corresponding spectral density in V/Hz$^{0.5}$. The governing equations of the CVA circuit described in Fig. 1 are the following:

(1) Ohm's law between A and B:

$$e'_{n+} + e'_{R_1} - R_1 I_1 + V_1 = 0, \tag{1}$$

(2) Ohm's law between B and C:

$$e'_{n+} = V_w - R_F I_F + e'_{R_F}, \tag{2}$$

(3) Kirchoff's law at B:

$$I_F + i'_{n-} = I_1, \tag{3}$$

(4) Ohm's law between C and D:

$$V_w = R_w I_w - e'_{R_w}, \tag{4}$$

(5) Ohm's law between C and E:

$$V_w = Z_a I_a - e'_{R_{2a}}, \tag{5}$$

(6) Ohm's law between S and C:

$$V_s = V_w + Z_b I_2 + e'_{R_2}, \tag{6}$$

(7) Kirchoff's law at C:

$$I_2 = I_a + I_w + I_F. \tag{7}$$

C. Electronic noise in the constant voltage anemometer

Using Eqs. (1)–(3), the wire voltage V_w can be written as

$$V_w = \frac{R_F}{R_1} V_1 + e'_n, \tag{8}$$

where

$$e'_n = \left(\frac{R_F}{R_1} + 1\right) e'_{n+} + \frac{R_F}{R_1} e'_{R_1} - R_F i'_{n-} - e'_{R_F}. \tag{9}$$

Equation (8) shows that the wire voltage V_w is held constant by the circuit, except for small voltage fluctuation e'_n due to electric noise in the different components.

An expression of the output voltage V_s as a function of V_w can be obtained by combining Eqs. (2) and (4)–(7). This gives

$$V_s = \left(1 + \frac{Z_b}{R_F} + \frac{Z_b}{Z_a} + \frac{Z_b}{R_w}\right) V_w + Z_b$$
$$\times \left(-\frac{e'_{n+}}{R_F} + \frac{e'_{R_{2a}}}{Z_a} + \frac{e'_{R_w}}{R_w} + \frac{e'_{R_F}}{R_F}\right) + e'_{R_2}. \quad (10)$$

We now perform a small perturbation analysis of Eq. (10), bearing in mind that the different noise sources can already by considered as small voltage perturbations. This yields

$$\nu'_s = \left(1 + \frac{Z_b}{R_F} + \frac{Z_b}{Z_a} + \frac{Z_b}{R_w}\right)\nu'_w - \frac{Z_b}{R_w}I_w r'_w + Z_b$$
$$\times \left(-\frac{e'_{n+}}{R_F} + \frac{e'_{R_{2a}}}{Z_a} + \frac{e'_{R_w}}{R_w} + \frac{e'_{R_F}}{R_F}\right) + e'_{R_2}. \quad (11)$$

This expression of the fluctuating output voltage ν'_s can be seen as the "noisy" counterpart of Eq. (3) in Ref. 2.

For frequencies lower than the cutoff of the anemometer, we can assume that V_w is held constant, except for the fluctuating noise voltage e'_n of Eq. (8). Inserting $\nu'_w = e'_n$ in Eq. (11) yields

$$\nu'_s = (\nu'_s)_t + (\nu'_s)_n, \quad (12)$$

where

$$(\nu'_s)_t = -\frac{Z_b}{R_w}I_w r'_w \quad (13)$$

is the fluctuating output voltage due to flow fluctuations, and where

$$(\nu'_s)_n = \left(1 + \frac{Z_b}{Z_a} + \frac{Z_b}{R_F} + \frac{Z_b}{R_w}\right)$$
$$\times \left[\left(\frac{R_F}{R_1} + 1\right)e'_{n+} + \frac{R_F}{R_1}e'_{R_1} - R_F i'_{n-} - e'_{R_F}\right]$$
$$+ Z_b \left(-\frac{e'_{n+}}{R_F} + \frac{e'_{R_{2a}}}{Z_a} + \frac{e'_{R_w}}{R_w} + \frac{e'_{R_F}}{R_F}\right) + e'_{R_2} \quad (14)$$

is the fluctuating output voltage caused by electronic noise in the components of the circuit. Reordering the different sources of noise, the expression of $(\nu'_s)_n$ can be written in the form:

$$(\nu'_s)_n = A \cdot e'_{n+} + B \cdot e'_{R_1} + C \cdot e'_{R_F} + D \cdot R_F \cdot i'_{n-} + E \cdot e'_{R_w}$$
$$+ F \cdot e'_{R_{2a}} + e'_{R_2}, \quad (15)$$

where

$$A = \left(1 + \frac{R_F}{R_1}\right)\left(1 + \frac{Z_b}{R_F} + \frac{Z_b}{Z_a} + \frac{Z_b}{R_w}\right) - \frac{Z_b}{R_F},$$

$$B = \frac{R_F}{R_1}\left(1 + \frac{Z_b}{R_F} + \frac{Z_b}{Z_a} + \frac{Z_b}{R_w}\right),$$

$$C = -\left(1 + \frac{Z_b}{Z_a} + \frac{Z_b}{R_w}\right),$$

$$D = -\left(1 + \frac{Z_b}{R_F} + \frac{Z_b}{Z_a} + \frac{Z_b}{R_w}\right),$$

$$E = \frac{Z_b}{R_w},$$

$$F = \frac{Z_b}{Z_a}.$$

The quantity $(\nu'_s)_n$ represents the noise voltage at the CVA output assuming that the op-amp works ideally up to an infinite frequency. In reality, at high frequency, the circuit gain will decrease because of the finite bandwidth of the system. This decrease in gain will affect the output voltage fluctuation $(\nu'_s)_n$ due to the noise, as well as the output voltage fluctuation $(\nu'_s)_t$ due to fluctuations in the flow. Hence, in a real system, a damping term must be added to Eqs. (13) and (15) to account for the decrease in gain.

According to Sarma,[2] a CVA behaves like a second-order system with a natural frequency f_n and a damping ratio ξ. f_n and ξ depend on the gain–bandwidth product of the op-amp as well as on R_2, R_w, T_c, and R_d. In addition, the CVA output is filtered by a fourth-order Butterworh filter to reduce aliasing when digitizing the output signals. The cutoff frequency f_{Bw} of this filter is higher than the natural frequency f_n of the CVA circuit itself. As a consequence, the damping term which needs to be added to Eqs. (13) and (15) may be written as

$$D(s) = \frac{B^{(4)}_{f_{Bw}}(s)}{(s/(2\pi f_n))^2 + 2\xi(s/(2\pi f_n)) + 1}, \quad (16)$$

where $B^{(4)}_{f_{Bw}}(s)$ is the transfer function of the Butterworth filter.

D. Simplified expression of $(\nu'_s)_n$

Equation (15), together with the damping term defined by Eq. (16), is an expression of the fluctuating output voltage of the CVA caused by the different sources of noise in the circuit. Although related quantities like the root mean square (rms) or the power spectral density (PSD) of $(\nu'_s)_n$ can be easily computed from Eq. (15) on a personal computer, it is helpful to simplify this expression to gain more insight into the parameters that mostly affect the signal-to-noise ratio.

The first step consists of noticing that R_F is larger than both R_w and R_{2a}, so that it is possible to neglect the terms in Z_b/R_F in Eq. (15). The expression of $(\nu'_s)_n$ then becomes

$$(\nu'_s)_n \simeq \left(1 + \frac{Z_b}{Z_a} + \frac{Z_b}{R_w}\right)e'_n + \frac{Z_b}{R_w}e'_{R_w} + \frac{Z_b}{Z_a}e'_{R_{2a}} + e'_{R_2}. \quad (17)$$

In the second step, the last three terms on the right-hand side (rhs) of Eq. (17) are found to be negligible compared to the first one, so that

$$(\nu'_s)_n \simeq \left(1 + \frac{Z_b}{Z_a} + \frac{Z_b}{R_w}\right)e'_n. \quad (18)$$

Equation (18) is an approximation of $(\nu'_s)_n$ that is much more tractable than the original expression (15). The term e'_n
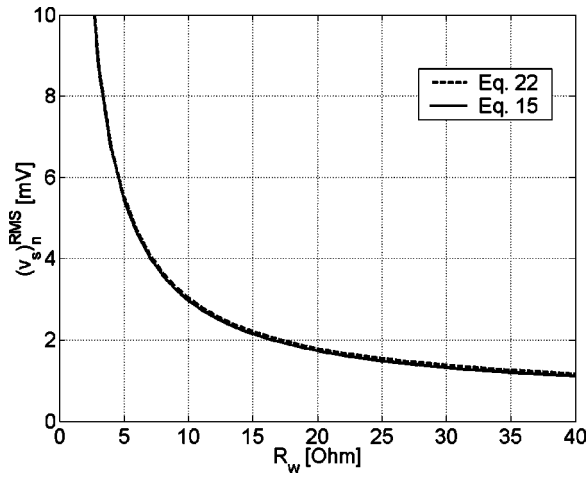
FIG. 2. Theoretical rms of CVA noise voltage in the bandwidth 1–400 kHz.

[defined by Eq. (9)] is a white noise source that depends only on the resistors R_F and R_1, and on the noise model of the op-amp.

When $f \gg 1/(2\pi T_c)$, one can assume that $Z_a \simeq R_{2a}$ and $Z_b \simeq 2\pi R_2 T_c jf$ so that Eq. (18) can be further simplified to give

$$(\nu'_s)_n \simeq 2\pi R_2 T_c jf \left(\frac{1}{R_{2a}} + \frac{1}{R_w} \right) e'_n. \qquad (19)$$

Thus, the PSD of the noise signal rises like f^2 at high frequency, like in the CCA and the CTA.[7,10] In addition, it is interesting to notice that the noise signal does not directly depend on V_w.

E. Estimation of the noise root-mean square

Since the most energetic part of the noise spectrum will be present at high frequency, the noise rms can be obtained by squaring Eq. (19) and integrating it between two frequencies f_1 and f_2 that are lower than the natural frequency f_n. This yields

$$\overline{((\nu'_s)_n)^2} = \int_{f_1}^{f_2} 4\pi^2 R_2^2 T_c^2 f^2 \left(\frac{1}{R_{2a}} + \frac{1}{R_w} \right)^2 e_n^2 \, df, \qquad (20)$$

The spectral density e_n of the input white noise can be obtained from Eq. (9) by assuming that the different noise sources are uncorrelated:

$$e_n^2 = \left(1 + \frac{R_F}{R_1} \right)^2 e_{n+}^2 + \left(\frac{R_F}{R_1} \right)^2 e_{R_1}^2 + R_F^2 i_{n-}^2 + e_{R_F}^2. \qquad (21)$$

Using the notation $(\nu_s)_n^{\text{rms}} = \sqrt{\overline{((\nu'_s)_n)^2}}$, one can finally write

$$(\nu_s)_n^{\text{rms}} \simeq 2\pi R_2 T_c \left(\frac{1}{R_{2a}} + \frac{1}{R_w} \right) \sqrt{\frac{f_2^3 - f_1^3}{3}} \, e_n. \qquad (22)$$

A plot of the noise rms against the wire resistance R_w is presented in Fig. 2. The solid line in Fig. 2 was obtained by integrating the original expression (15), whereas the dotted line was obtained using the simplified expression (22). The PSD was integrated between $f_1 = 1$ kHz and $f_2 = 400$ kHz and typical values were used for the resistors in the CVA: $R_1 = 1500\,\Omega$, $R_F = 300\,\Omega$, $R_{2a} = 50\,\Omega$, $R_2 = 100\,\Omega$, and T_c

$= 0.1$ ms. The amplifier noise characteristics were assumed to be typical for recent low-noise high-performance op-amps: $e_{n+} = 1.0$ nV/Hz$^{0.5}$ and $i_{n-} = 0.8$ pA/Hz$^{0.5}$. According to Eq. (21), these values yield a white noise spectral density of $e_n = 2.7$ nV/Hz$^{0.5}$.

It can be seen in Fig. 2 that the two curves are very close to another, justifying the simplifications made above. One advantage of Eq. (22) is that it shows well the functional relation between the noise rms and R_w. In particular, plotting $R_w \cdot (\nu_s)_n^{\text{rms}}$ should give a straight line, the slope and intercept of which only depend on CVA parameters like R_2, R_{2a}, T_c, the bandwidth of interest, and only one noise-related quantity. This provides a convenient way to check the validity of the present theory against experimental data, as will be done in a further section.

F. Signal-to-noise ratio

The signal-to-noise ratio in the CVA can be obtained by comparing the output voltage $(\nu'_s)_t$ that is caused by fluctuations in the flow to the output voltage $(\nu'_s)_n$ due to electronic noise. According to Comte-Bellot,[16] the voltage fluctuation $(\nu'_s)_t$ caused by a velocity fluctuation u' at frequency f can be written as

$$(\nu'_s)_t = \frac{1 + 2j\pi f T_c}{1 + 2j\pi f M_{\text{CVA}}} \frac{a_w}{2(1 + 2a_w)} \frac{B\sqrt{U}}{A + B\sqrt{U}} \frac{u'}{U} V_s, \qquad (23)$$

where U is the mean velocity, and a_w is the corresponding wire overheat ratio, A and B are the "constants" (depending on the wire) in the classic King's form of the heat exchange law of the wire $R_w I_w^2/(R_w - R_a) = A + B\sqrt{U}$.

In practice, electronic noise is an important issue only for frequencies higher than the wire natural frequency $1/(2\pi M_{\text{CVA}})$ [which is usually close to the frequency $1/(2\pi T_c)$ of the compensation network] and lower than the natural frequency f_n. Thus, the first factor in the rhs of Eq. (23) may be simplified by T_c/M_{CVA}. In addition, the mean output voltage $V_s = (1 + R_2/R_F + R_2/R_w)V_w$ may be approached by $V_s \simeq V_w R_2/R_w$. Using these simplifications, Eq. (23) can be written as

$$(\nu'_s)_t = \frac{T_c}{M_{\text{CVA}}} \frac{a_w}{2(1 + 2a_w)} \frac{V_w R_2}{R_w} \frac{B\sqrt{U}}{A + B\sqrt{U}} \frac{u'}{U}. \qquad (24)$$

At the same frequency, the amplitude $(\nu'_s)_n$ caused by the white noise voltage fluctuation e'_n in the circuit can be obtained from Eq. (19):

$$(\nu'_s)_n = 2\pi f R_2 T_c \left(\frac{1}{R_{2a}} + \frac{1}{R_w} \right) e'_n. \qquad (25)$$

Dividing Eqs. (24) and (25), and using the spectral densities u and e_n as explained at the beginning of Sec. II B yield an expression of the signal-to-noise ratio:

$(\text{SNR})_{\text{CVA}}$

$$= \frac{(\nu'_s)_t}{(\nu'_s)_n}$$

$$= \frac{1}{2\pi f M_{\text{CVA}}} \frac{R_{2a}}{R_{2a}+R_w} \frac{a_w}{2(1+2a_w)} \frac{B\sqrt{U}}{A+B\sqrt{U}} \frac{V_w}{e_n} \frac{u}{U}. \tag{26}$$

For high-speed flow, $B\sqrt{U}/(A+B\sqrt{U})\simeq 1$ and expression (26) may be approached by

$$(\text{SNR})_{\text{CVA}} = \frac{1}{2\pi f M_{\text{CVA}}} \frac{R_{2a}}{R_{2a}+R_w} \frac{a_w}{2(1+2a_w)} \frac{V_w}{e_n} \frac{u}{U}. \tag{27}$$

Equation (27) expresses the signal-to-noise ratio in the CVA at a frequency f in terms of explicit quantities that are usually known to the experimentalist. In particular, it shows that the signal-to-noise ratio decreases if the frequency increases, if the noise level in the circuit increases, or if the level of turbulence decreases. For low turbulent signals, the maximum usable frequency may, for example, be calculated from Eq. (27) by putting $(\text{SNR})_{\text{CVA}}=1$ and solving for f.

For the M_{CVA} value, a useful relation has been established by Comte-Bellot and Sarma:[3]

$$M_{\text{CVA}} = \frac{1+a_w}{1+2a_w} \frac{d^2\rho_w c_w}{4k_a} \frac{1}{A'+B'\sqrt{\text{Re}_d}}, \tag{28}$$

where d is the wire diameter, ρ_w and c_w the density and specific heat of the wire material, k_a is the thermal conductivity of the ambient fluid at temperature T_a, Re_d is the wire Reynolds number, and A' and B' the constants in the general nondimensional heat transfer law of the wire: $Nu_d=A'+B'\sqrt{\text{Re}_d}$, where $A'\simeq 0$ at high velocity and $B'\simeq 0.56$. Taking Eq. (28) into account in Eq. 27, it can be shown that the signal-to-noise ratio can be improved by operating the wire at a high overheat ratio and using a thin wire to minimize thermal inertia.

III. EXPERIMENTAL RESULTS

A. Experimental procedure

Measurements of electronic noise were performed on the CVA prototype CV01 manufactured by Tao Systems Inc. (Williamsburg, VA) To cover a wide range of R_w, standard resistors as well as two hot wires were used. The hot wires were standard tungsten wires, respectively, 2.5 μm and 5 μm in diameter that were spot welded to the prongs of a commercial probe (Dantec). Most of the data were acquired with a Textronics eight-bit digital oscilloscope at 2.5 MHz and 5 MHz sampling frequency. For special measurements that will be detailed below, a HP35665A digital oscilloscope with 16-bit resolution and a sampling frequency of 262 kHz was used. The time constant T_c of the RC network was set to $T_c=0.098$ ms, a value used in most of the CVA experiments in supersonic flows.[3,5] With those settings, the natural frequency of the CVA circuit was $f_n=470$ kHz and the cutoff frequency of the Butterworth filter was set to f_{Bw}
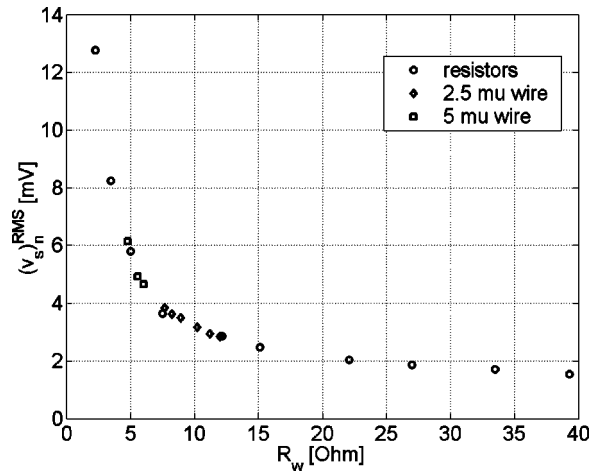

FIG. 3. Experimental rms of CVA noise in the bandwidth 1–400 kHz.

$=670$ kHz. The electronic noise in the circuit was obtained by directly measuring the fluctuating output voltage of the CVA. When resistors were used, this method of operation is obvious. When real hot wires were used, care was taken to put the wire in very still air, in order to limit the contribution of the output signal due to flow fluctuations. Nevertheless, natural convection over the hot wire was unavoidable but contributed to the signal at a frequency much lower than the frequency of interest in the present measurements.

B. Noise root-mean square

Figure 3 presents a plot of the measured value of the noise rms $(\nu_s)_n^{\text{rms}}$. In order to compare these data with the simple expression (22), the rms was computed within 1 kHz and 400 kHz to ensure that only frequencies lower than the natural frequency f_n were taken into account. For the data obtained with the resistors, it was checked that the noise rms does not depend on V_w, in accordance with the theory. For the hot wires, a change of V_w resulted in a change of R_w and a corresponding change of the noise rms. It can be seen in Fig. 3 that the output voltage due to electronic noise decreases with the wire resistance, as predicted by the theory. When the sensor is removed from the circuit ($R_w=\infty$), $(\nu_s)_n^{\text{rms}}$ goes down to the lower limit 1.2 mV. The trend of the experimental data is very similar to the theoretical curves reported in Fig. 2 and shows that one can advantageously estimate an upper limit of the electronic noise by using the results of the unheated wire.

In order to perform a more quantitative comparison with the theory, Fig. 4 presents a plot of $(\nu_s)_n^{\text{rms}}$ times R_w. It can be seen in Fig. 4 that the measured data can well be fitted to a straight line, independent of what type of sensor is used. This is consistent with Eq. (22). Identifying the parameters of the linear fit with Eq. (22), and bearing in mind that the quantities $R_2=100\,\Omega$ and $T_c=0.098$ ms are known, one obtains a value of $R_{2a}\simeq 20\,\Omega$ and a white noise level of $e_n=2.6$ nV/Hz$^{0.5}$. This value of e_n is similar to the estimate presented in Sec. II E and the present measurements therefore agree very well with the theory derived above.
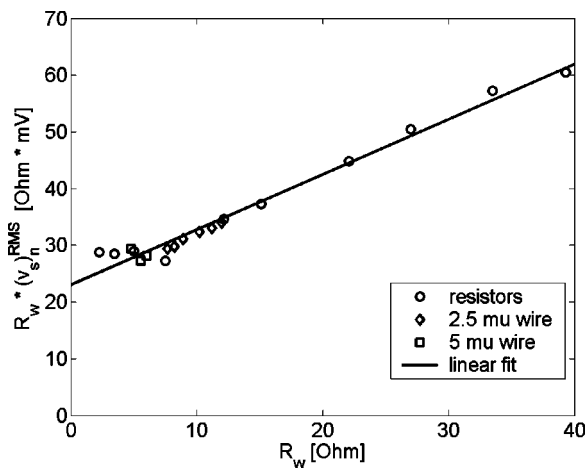
FIG. 4. Product of noise rms (bandwidth: 1–400 kHz) with wire resistance.

C. Noise spectra

Figure 5 shows a comparison between the PSD of the output noise calculated using the proposed theory and the measured data for two values of R_w. The data corresponding to $R_w = 7.7 \, \Omega$ were obtained with the 5 μm wire and a sampling rate of $f_s = 5$ MHz. For $R_w = 39 \, \Omega$, a standard resistor was used and the sampling rate was $f_s = 2.5$ MHz. The theoretical PSDs were calculated using expression (18), taking into account the damping term and the Butterworth response [Eq. (16)]. The values $R_{2a} \simeq 20 \, \Omega$ and $e_n = 2.6$ nV/Hz$^{0.5}$ obtained in last section were used.

It can be seen in Fig. 5 that the theoretical curves are flat for $f < 1/(2\pi T_c)$ and rise like f^2 when $f > 1/(2\pi T_c)$. On the other hand, the experimental spectra show this f^2 rise only at high frequencies. For frequencies lower than 40 kHz, the experimental curve corresponding to $R_w = 39 \, \Omega$ is much higher than the theoretical curve, and actually decreases with the frequency for $f < 10$ kHz. The same phenomenon appears for $R_w = 7.7 \, \Omega$, but the f^2 trend is present in a larger bandwidth. Nevertheless, the calculated PSDs are very close to
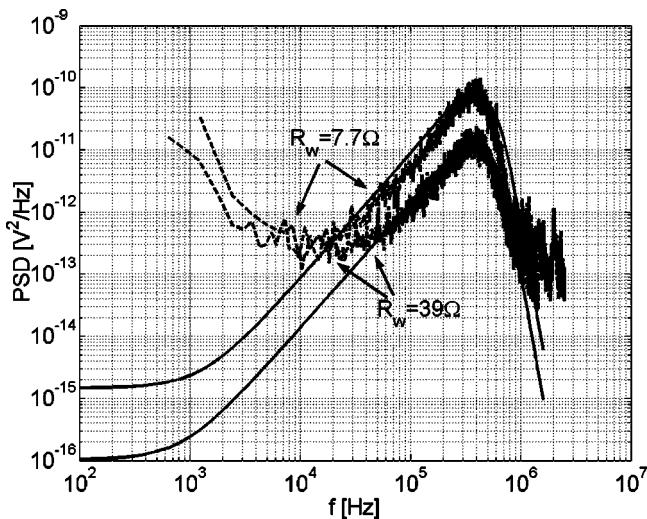

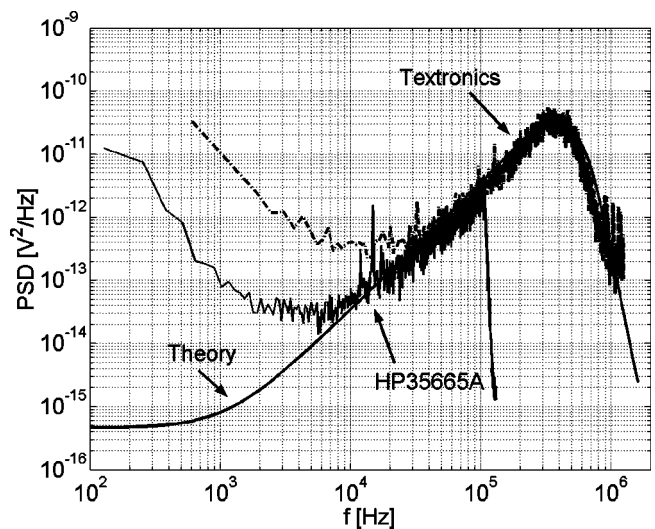FIG. 5. Comparison between theoretical and measured PSD; solid line: Theory, dashed line: Experiments.

FIG. 6. Comparison between theoretical and measured PSD using Textronics and HP35665A digital oscilloscopes; solid line: HP35665A, dashed line: Textronics, smooth solid line: Theory.

the experimental curves in the largest and most energetic part of the spectrum.

The mismatch between theory and experiments may be related to data acquisition issues. It can be seen in Fig. 5 that the PSD level at very high and low frequencies is actually higher than the theoretical curves. At high frequencies, the experimental spectra seem to reach a plateau for $f > 1$ MHz, and their shape is very irregular. This phenomenon is due to the inability of the digital oscilloscope to resolve the low level of fluctuations present at these frequencies. In fact, an examination of Fig. 5 reveals that a PSD level of 10^{-13} V^2/Hz is the lowest signal that can be resolved by the system. Similarly, the low PSD level at low frequency cannot be resolved. In addition, it is interesting to notice the presence of peaks in the experimental spectra at high frequency ($f \simeq 2$–5 MHz). These peaks can influence the measured spectra at low frequency through the phenomenon of aliasing, and thus artificially increase the PSD level at low frequency.

To illustrate this phenomenon, measurements were performed with the HP35665A digital oscilloscope in addition to the standard data obtained with the Textronics. The sampling frequency of the HP35665A is limited to $f_s = 262$ kHz, but a very sharp antialiasing filter is included in the circuit (-72 dB/oct). In addition, the HP35665A is a 16-bit system, in comparison to the eight bits of the Textronics. A comparison of the spectra obtained with the two acquisition systems is shown in Fig. 6. The measurements were performed with a resistor of $R_w = 15 \, \Omega$. The solid line in Fig. 6 shows the data obtained with the HP35665A, whereas the dotted line shows the data measured with the Textronics. In addition, the theoretical PSD is also shown (smooth solid line). It can be seen in Fig. 6 that the PSD measured with the HP35665A fits the theoretical curve for almost a decade longer than with the Textronics.

IV. DISCUSSION

A theory was proposed to compute the signal-to-noise ratio in the CVA. The theory is based on the comparison of

output voltage caused by fluctuations in the flow and output voltage due to the electronic noise coming from the op-amp and the resistances in the circuit. Measurements of electronic noise in a CVA prototype confirmed the proposed theory in a broad range of frequencies.

An examination of Eq. (27) reveals that the signal-to-noise ratio can be improved by operating the wire at a high overheat and using a thin wire to minimize thermal inertia. In addition, the signal-to-noise ratio is large at low frequencies and when the level of fluctuations in the flow is high. In fact, these requirements are similar to those proposed by Fingerson[17] for other types of anemometers. Another very important parameter that drives the signal-to-noise ratio is the overall noise level e_n' present in the electronic circuitry, given by Eq. (9). This level should be minimized as much as possible to improve the signal-to-noise ratio. Some CVA characteristics also have to be taken into account as can be seen in Eq. (22).

Finally, it should be noted that experimental measurements of electronic noise in hot-wire anemometers are not easy in terms of a data acquisition technique. Although measurements of noise may not be considered to be very exciting for the fluid dynamicist, the same type of issues may appear for measurements of very low flow fluctuations, for example in the free stream of high-speed wind tunnels.[5,9] Therefore, the particular point of aliasing will now be discussed.

One of the advantages of CVA is its large bandwidth. As a consequence, a high sampling rate is needed to measure the fluctuations of its output voltage without aliasing. Of course, the same type of requirement is necessary for standard flow fluctuations but in the case of noise, the energetic part of the spectrum is present at high frequency and its spectrum increases like f^2. On the contrary, the spectrum of turbulent flows decreases with the frequency. Therefore, aliasing is a more critical issue for noise measurements since high-frequency fluctuations above the Nyquist frequency may be folded back and alter significantly the low-frequency part of the spectrum. In addition, the resolution of digital data acquisition systems usually decreases at a very high frequency so that the measured PSD level near the Nyquist frequency may be higher than the physical noise spectrum. These two interrelated phenomena are believed to be the cause of the difference between the noise spectra measured with two different data acquisition systems in Fig. 6.

To illustrate the issue of aliasing, spectra of electronic noise were computed using the theory presented above. In addition, the effect of aliasing was simulated by adding the contribution of the PSD present between the sampling frequency f_s and the Nyquist frequency $f_s/2$. The results are given in Fig. 7. The spectrum corresponding to a sampling frequency of $f_s = 2.5$ MHz follows the theoretical curve almost up to the Nyquist frequency, so that no practical effect of aliasing is expected at this sampling rate. For $f_s = 1$ MHz, however, the simulated spectrum is heavily distorted by aliasing: In particular, the low-frequency part of the spectrum cannot be resolved and the slope of the spectrum is lower than the theoretical f^2 slope for frequencies lower that 100 kHz. Finally, for $f_s = 0.5$ MHz, the simulated spectrum is completely in error.
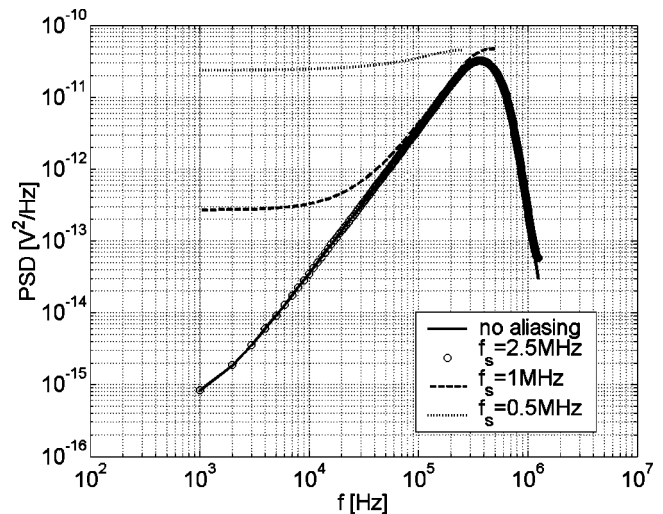

FIG. 7. Effect of aliasing on electronic noise measurement.

The authors believe that the effect of aliasing combined with the usually poor resolution of digital oscilloscopes at a high frequency are responsible for the differences in noise spectra presented in earlier references.[3,5] In addition, these results show the need to use a very sharp filter when flow fluctuations are of interest in a limited bandwidth only.

ACKNOWLEDGMENTS

[1] G. R. Sarma, U.S. Patent No. 5,074,147 (1991).
[2] G. R. Sarma, Rev. Sci. Instrum. **69**, 2385 (1998).
[3] G. Comte-Bellot and G. R. Sarma, AIAA J. **39**, 261 (2001).
[4] J. T. Lachowicz, N. Chokani, and S. P. Wilkinson, AIAA J. **34**, 2496 (1996).
[5] J. Weiss, H. Knauss, S. Wagner, N. Chokani, G. Comte-Bellot, and A. D. Kosinov, Proceedings of the 41st AIAA Aerospace Sciences Meeting and Exhibit (AIAA, 2003), paper 2003-0976.
[6] J. Norris and N. Chokani, AIAA J. **41**, 1619 (2003).
[7] P. Freymuth, Rev. Sci. Instrum. **39**, 550 (1968).
[8] P. Freymuth, J. Phys. E **11**, 915 (1978).
[9] S. G. Saddoughi and S. V. Veeravalli, Meas. Sci. Technol. **7**, 1297 (1996).
[10] P. Freymuth and L. M. Fingerson, Meas. Sci. Technol. **8**, 115 (1997).
[11] J. Weiss, H. Knauss, and S. Wagner, Rev. Sci. Instrum. **72**, 1904 (2001).
[12] D. Bestion, J. Gaviglio, and J. P. Bonnet, Rev. Sci. Instrum. **54**, 1513 (1983).
[13] The CVA has been shown to be far less susceptible to electromagnetic noise than other types of anemometers [J. T. Lachowicz, N. Chokani, and S. P. Wilkinson, AIAA J. **34**, 2496 (1996)]. This type of noise will not be considered in the present article.
[14] G. Asch et al., Acquisition de données. Du capteur à l'ordinateur (Dunod, Paris, 1999).
[15] M. Steffes, Burr-Brown Application Bulletin AB-103 (1996).
[16] G. Comte-Bellot, in Handbook of Fluid Dynamics, edited by R. W. Johnson (CRC Press, Boca Raton, 1998), Chap. 34.
[17] L. M. Fingerson, Rev. Sci. Instrum. **65**, 285 (1994).